Computational and Theoretical Chemistry 1005 (2013) 1–8

Contents lists available at SciVerse ScienceDirect

Computational and Theoretical Chemistry

journal homepage: www.elsevier.com/locate/comptc

Polarizability, chemical hardness and ionization potential as descriptors to understand the mechanism of double proton transfer in acetamide dimer

Hasibul Beg, Sankar Prasad De, Sankarlal Ash, Debasish Das, Ajay Misra *

Department of Chemistry and Chemical Technology, Vidyasagar University, Midnapore 721 102, WB, India

ARTICLE INFO

Article history:
Received 13 August 2012
Received in revised form 31 October 2012
Accepted 31 October 2012
Available online 24 November 2012

Keywords:
Double proton transfer (DPT)
DFT
TS
IP
Polarizability
Chemical hardness

ABSTRACT

The double proton transfer mechanism in the acetamide dimer is examined in terms of the energy profile, reaction force, chemical hardness, average polarizability, ionization potential, chemical potential and interaction energies using HF as well as density functional theory based approach. The energy profile for the activation process of acetamide dimer to the imino ether product is obtained using B3LYP function and is in agreement with the results of the other methods. To test the validity of the reaction mechanism, the intrinsic reaction coordinate (IRC) calculation is performed at the B3LYP level of theory. The results show that the reaction starts with a structural rearrangement, where the two dimers approach each other, and through the transition state (TS) product is obtained. This structural rearrangement to the activation barrier steers the activation process. During the course of double proton transfer reaction in acetamide dimer (AAD) we observe that the ionization potential (IP) is inversely related with average polarizability (α_{av}) and linearly related with chemical hardness (η). We also observe that the use of N—H distance as proton transfer co-ordinate nicely explain the reaction energy profile and it is computationally less expensive than the IRC method.

1. Introduction

Proton-transfer reactions are one of the most important processes in chemistry and biochemistry. The understanding of several issues of reactivity compelling such reactions has been the subject of extensive research from both experimental and theoretical point of view [1–7]. Double proton transfer in DNA base pairs is a commonly cited example. Amide dimerization involving intermolecular proton transfer is a chemical process relevant to understanding the formation of protein structures and many processes of molecular recognition in polar and apolar solvents [8]. In fact, the dimerization of cis amides is probably similar to the H-bonding pattern responsible for recognition of nucleic-acid bases. Owing to the chemical and biochemical implications of amide–amide recognition, extensive research effort has been devoted to determine the free energy of dimerization of cis and trans amides in different solvents [9]. In most cases the association was examined from the changes in the infrared spectra of amide monomers and dimmers [9]. There are also a large number of theoretical studies on this topic [10] which address the free energy of dimerization of amides in the gas phase, and also to estimate the effect of the environment in dimerization process. Most models of amide dimerization assume that this interaction occurs mainly through H-bonding, especially for the cis amides.

Most interest in studying the acetamide (CH3CONH2) molecule stems from its importance as a model of peptide bonds in biological molecules [11] in addition to its carcinogenic effects [12]. Acetamide constitutes a dominant N-containing product from the fragmentation of soil organic matter [13], biomass [14], sewage sludge [15] and explosives [16]. It is believed that the major source of acetamide comes from the rupture of the amino polysaccharide linkages present in chitin, that is, the second largest structural block in biomass [17]. Acetamide is also produced in appreciable concentrations from the pyrolysis of peptides [18], fungi [17], bacteria cells [19], humic and fluvic acids [12].

Numerous studies have been devoted to investigate the hydrogen bond (HB) features in the natural phenomena, especially in biological systems. Indeed, HB plays a major role in determining the structure of polypeptides in proteins. Since the structures of macromolecular proteins in living systems are very complex, studying the simplest models having the major characteristic of proteins is an advantage in the investigation of hydrogen bond properties in these structures. Acetamide which has a single peptide group (O=C—NH), is the simplest model system of peptide linkage in proteins and polypeptides. Acetamide and some of its derivatives are capable of contributing to N—H...O=C and CH...O=C types of HB interactions. A variety of theoretical and experimental methods are employed to obtain information about

* Corresponding author. Tel.: +91 8967 986988; fax: +91 3222 275329.
E-mail address: ajaymsr@yahoo.co.in (A. Misra).

2210-271X/$ - see front matter © 2012 Elsevier B.V. All rights reserved.
http://dx.doi.org/10.1016/j.comptc.2012.10.023

the properties of HB interactions. However, nuclear quadrupole resonance (NQR) and nuclear magnetic resonance (NMR) spectroscopies are among the most efficient techniques for this purpose [20,21]. The hydrogen bond properties of peptide group in crystalline structure of acetamide are studied recently [22a]. The most stable, symmetric dimer of acetamide is clearly assigned in the gas phase [22b]. Resonance Raman spectra of N-methylacetamide (NMA) and its isotopic derivatives had been reported for the vapor phase [22c]. Effects of intermolecular hydrogen-bonding interactions on N-methylacetamide (NMA) are studied by matrix-isolation infrared (IR) spectroscopy and ab initio molecular orbital calculations in the gas phase [22d]. Ab initio molecular orbital calculations and Monte Carlo statistical mechanics simulations have been used to study the cis–trans equilibrium for N-methylacetamide (NMA) in the gas phase [22e]. N—H···O hydrogen bonding properties of linear H-bonded acetamide clusters were theoretically investigated [22f]. The double proton transfers in the formamide dimer were characterized computationally by combining density functional theory and ab initio methods in the gas phase [22g]. Despite the extensive works done on acetamide, the double proton reaction path in terms of its electronic properties is yet to be explored.

During the last few years extensive studies were performed on the hardness (η), softness (S), and polarizability (α) of time-dependent systems [23]. These studies include chemical reactions as well as intramolecular vibrations and rotations [23,24]. From detailed theoretical studies it has been found that "there seems to be a rule of nature that molecules arrange themselves so as to be as hard as possible" (maximum hardness principle, MHP) [23]. It was also stated that "the natural direction of evolution of any system is toward a state of minimum polarizability" (minimum polarizability principle, MPP) [25,26]. The latter principle can be thought of as a consequence of the inverse relationship between α and η and the validity of the maximum hardness principle. In this Communication we verify a similar principle for ionization potential which can be stated as "a stable configuration/conformation of a molecule is associated with a maximum value of the ionization potential."

In this study, detailed theoretical investigations of the homogeneous gas-phase double proton transfer of acetamide dimer are carried out. Our primary aim is to account qualitatively the role of chemical potential, polarizability, hardness, ionization potential, interaction energy in the overall mechanism of double proton transfer in acetamide to form dimer. It is hoped that this study will provide kinetic input for the reaction that account satisfactorily for the double proton transfer in acetamide as a model compound of dimmers which are formed through the double hydrogen bond.

2. Theoretical background

Quantum chemical methods have been proven to be a very useful tool to study chemical systems stabilized by hydrogen bonds. The two theoretical methodologies most frequently used are the Density Functional Theory (DFT) and the second order Møller–Plesset Perturbation Theory (MP2). In the framework of density functional theory (DFT) global descriptors of chemical reactivity correspond to global responses of systems to global perturbations (for instance, changes in the number of electrons N), whereas the external potential $V(r)$ remains constant. Among such types of indexes, chemical potential (μ), chemical hardness (η) and softness (S) can be used as complementary tools in the description of thermodynamic aspects of chemical reactivity. The first order partial derivatives of total energy (E) with respect to the number of electrons (N) at constant external potential, $V(r)$, define chemical potential (μ) and the second partial derivatives of total energy (E) with respect to the number of electrons (N) at constant external potential, $V(r)$, define the global hardness (η) of the system [23–29].

$$\mu = (\partial E/\partial N)_{V(r)} \tag{1}$$

$$\eta = (\delta^2 E/\delta N^2)_{V(r)} \tag{2}$$

Operational schemes for the calculation of chemical hardness are based on a finite difference method and thus,

$$\mu \approx -1/2(IP + EA) \tag{3}$$

$$\eta \approx 1/2(IP - EA) \tag{4}$$

where IP = Ionization Potential and EA = Electron Affinity. Using the Koopmans' theorem in terms of the energies of highest occupied molecular orbital (E_{HOMO}) and lowest unoccupied molecular orbital (E_{LUMO}), the Eqs. (3) and (4) can be expressed as

$$\mu \approx 1/2(E_{\mathrm{HOMO}} + E_{\mathrm{LUMO}}) \tag{5}$$

$$\eta \approx 1/2(E_{\mathrm{LUMO}} - E_{\mathrm{HOMO}}) \tag{6}$$

These global quantities, as well as the mean polarizability values (α), have been found very useful and complementary tools for the description of chemical reactivity in connection with minimum polarizability and maximum hardness principles. The α_{av} has been calculated using the following expression.

$$\alpha_{av} = 1/3(\alpha_{xx} + \alpha_{yy} + \alpha_{zz}) \tag{7}$$

In connection with the global ideas of chemical reactivity, the transition structure can be characterized through its intrinsic properties, the energy barrier $\Delta E^* = [E\,(TS) - E(R)]$, the activation hardness $\Delta\eta^* = [\eta\,(TS) - \eta(R)]$ and the activation ionization potential $\Delta\mathrm{IP} = [\mathrm{IP}_{(\mathrm{TS})} - \mathrm{IP}_{(\mathrm{R})}]$. These activation values are defined simply as the difference between the TS property and that corresponds to the reactant.

For any chemical or physical process, the "reaction force" $\mathbf{F}(\mathbf{R}c)$ is given by

$$\mathbf{F}(\mathbf{R}c) = -\partial V(\mathrm{Rc})/\partial \mathrm{Rc}. \tag{8}$$

where V(Rc) is the potential energy of the system along the intrinsic reaction coordinate Rc [30].

2.1. 1computational details

All the ground-state structures of the Reactants, products and the transition states (TSs) are optimized using the Becke 3 parameter Lee–Yang–Parr (B3LYP) [31] hybrid density functional theory (DFT) at the 6-31G(d) level of basis set [32,33]. Frequency calculations are performed on the optimized structures to confirm that these structures belong to the lowest energy minima. We have performed the scan job on the potential energy profile for various (N---H---O) by changing N—H distances. Polarizabilities are calculated for each scan step at a frequency of 1064 nm corresponding to the Nd: YAG frequency proposed by Snijders and Baerends [34]. All the frequency dependent polarizabilities are computed using HF/6-31G(d) and DFT-B3LYP/6-31G(d) level of theory. It is important to note that results for calculations of polarizabilities are quite dependent on the level of exchange and correlations [35]. The HOMO and LUMO energies are also calculated for each scan step to establish the profile for the variation in the chemical hardness (η) with N—H bond distances. For the intermolecular double H-bonded complexes, the scans are performed by simultaneous, equivalent and opposite increases in N—H bond distances for both the H-bonds. The ground state optimized energy calculations for each scan point along N—H co-ordinate using the DFT level of theory are also done by MP2/6-311G(d,p) level of theory.

For all the optimized structures, the TS correspond to the asymmetric hydrogen bridged structures since the donor and the acceptor atoms are different. The donor atoms are nitrogen (N) of the amide (NH_2) group and the acceptor atoms are oxygen (O) of the ketonic (C=O) group for all the structures. At TS, N—H distance is 1.30 Å and O—H distance is 1.23 Å. Our frequency calculation on the optimized TS structure give single imaginary frequency. Then IRC calculations are performed by DFT-B3LYP/6-31G(d) level of theory and it supports the double proton transfer in acetamide during dimerization reaction. In IRC path the transition state connects the reactant and product. The electronic chemical potential was obtained from single point energy calculations of all structures along the reaction coordinate (r_{N-H}) employing 6-31G(d) basis set at different level of theory discussed in Section 3.2 in this article. Monomeric structures of AAD at different N—H distance are optimized by DFT-B3LYP/6-31G(d) level of theory and we have performed the energy calculation of all the structures using 6-31G(d) basis set at HF, DFT-B3LYP, MP2 & QCISD method. All the calculations are performed in Gaussian-09 package program.

3. Results and discussion

The double proton transfer of the acetamide dimer has been investigated here using several approaches. Ionization potential, polarizability, chemical hardness and chemical potential are used as quantum chemical reactivity descriptor to study the path of double proton transfer reaction in acetamide dimer. We have also studied the reaction force profile and interaction energy along the reaction co-ordinate.

3.1. Energy and reaction force

The kinetics of proton transfer reactions strictly depend on the detailed profile of the reaction barrier. According to classical transition-state theory, the rate of a reaction is controlled by the barrier height. Potential energy of double proton transfer in aecetamide dimer (AAD) along the proton transfer co-ordinate (N—H) are shown in Table 1. Our computed potential energy barrier for double proton transfer in AAD are 33.45 kcal mole^{-1} at HF, 20.39 kcal mole^{-1} at DFT-B3LYP, 16.19 kcal mole^{-1} at MP2 and 30 kcal mole^{-1} at QCISD method by using 6-31G(d) basis set in each case. These are considerably higher barrier for double proton transfer to occur in AAD and the product is 23.41 kcal mole^{-1}, 19.64 kcal mole^{-1}, 13.55 kcal mole^{-1} and 19.95 kcal mole^{-1} higher in energy ($\Delta E_{reaction}$) than the reactant at HF, DFT-B3LYP. MP2 and QCISD level of theory respectively. There is significant agreement between the patterns of variations of energies with N—H distances at several methods (Table 1). The primary disagreement appears only to lie in the activation barrier.

The reaction mechanism of the double proton transfer in acetamide was examined by the intrinsic reaction coordinate (IRC) between reactant and product at DFT-B3LYP/6-31G(d) level of theory. In IRC methodology the potential energy barrier for double proton transfer in AAD is 20.64 kcal mole^{-1} and the reaction energy ($\Delta E_{reaction}$) is 17.44 kcal mole^{-1}. These results are in close agreement with that in the proposed N—H distance as proton transfer co-ordinate using the same level of theory.

We have used the variation of reaction force [$\mathbf{F}(\mathbf{R}c)$] along the proton transfer co-ordinate to analyze the double proton transfer reaction in acetamide dimer, using DFT-B3LYP/6-31G(d) level of theory. The reaction force profile leads to interesting information about the double proton transfer of the acetamide dimer as shown in Fig. 1. Initially the reaction force decreases along the IRC path and then sharply until it reaches a minimum. This decrease is due to the decreasing intermolecular distance between the monomers and at the same time no change occurs in the N—H distance. The negative linear decrease of the reaction force implies a repulsion energy, which depends quadratically on the distance between the two monomers, suggesting an interaction similar to the one in a covalent chemical bond. The pronounced decrease near the minimum initiates the elongation of the N—H bond, which continues until the transition state and reaches into the product region. The change in the nature of the reaction force near the minimum together with the increasing N—H distance indicates the onset of an electronic redistribution.

The reaction force in the transition state region (A to C) crosses zero (B) and decreases linearly in the product region. The transition state region describes the trajectory of the hydrogen atom from the donor to acceptor atom keeping the distance between the donor nitrogen and the acceptor oxygen atom as constant. This process is dominated by electronic changes. In the product region (after C) the reaction force adopts again a linear behavior with almost fixed O—H distance and the two monomers are separated from each other. The much smaller structural rearrangements are required in the product region go in line with a product like transition state in accordance with the Hammond postulate. Plot of reaction force, $\mathbf{F}(\mathbf{R}c)$, as a function of increasing N—H distances (Fig. 2) also gives similar trend. Therefore, the use of N—H distance as a substitute of reaction co-ordinate can also be used to get a quick idea about the nature of potential energy profile for the dimerization of acetamide.

Table 1
Variations of energy (kcal/mol) with (N—H) distances at different level of theory.

r_{N-H} (Å)	HF/6-31G(d)	DFT-B3LYP/6-31G(d)	MP2/6-311G(d,p)	QCISD/6-31G(d)
1.05	−261022.3029	−262580.9738	−261932.5055	−261018.8516
1.1	−261016.2161	−262577.7735	−261928.6776	−261013.204
1.15	−261007.7447	−262574.0712	−261925.0381	−261007.7447
1.2	−260998.5203	−262568.4863	−261919.8925	−260998.4576
1.25	−260991.6177	−262564.0938	−261916.8177	−260991.6177
1.3	−260988.8567	−262560.5797	−261916.3157	−260988.8567
1.35	−260988.7939	−262560.7052	−261916.8177	−260988.7939
1.4	−260989.9234	−262561.6465	−261917.3197	−260989.9234
1.45	−260991.555	−262560.768	−261917.759	−260991.555
1.5	−260994.4415	−262561.27	−261918.01	−260994.4415
1.55	−260994.8808	−262561.4582	−261918.261	−260994.8808
1.6	−260995.0063	−262561.6465	−261918.512	−260994.9435
1.65	−260997.4535	−262561.7092	−261918.763	−260997.4535
1.7	−260998.3321	−262561.5837	−261918.8257	−260997.8301
1.75	−260998.8968	−262561.3327	−261918.9512	−260998.8968

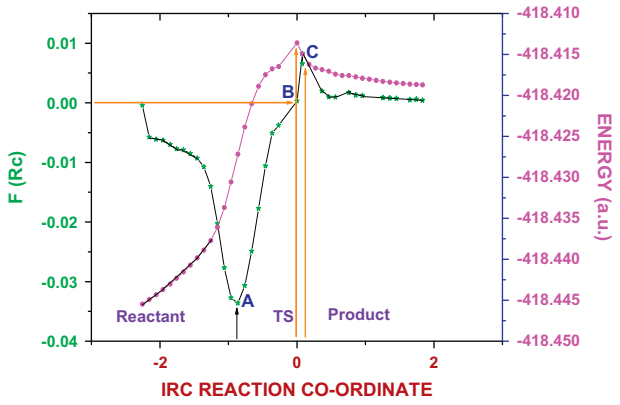

Fig. 1. Profile of the potential energy $V(\mathbf{R}c)$ and the reaction force $\mathbf{F}(\mathbf{R}c)$ along the intrinsic reaction coordinate, $\mathbf{R}c$, at DFT-B3LYP/6-31G(d) level of theory.

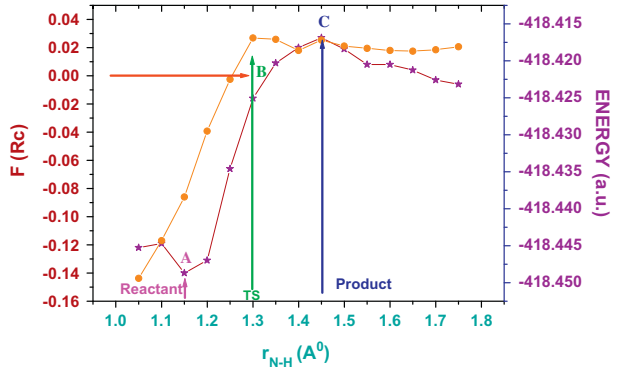

Fig. 2. Profile of the potential energy $V(\mathbf{R}c)$ and the reaction force $\mathbf{F}(\mathbf{R}c)$ with increasing N—H bond distances at DFT-B3LYP/6-31G(d) level of theory.

3.2. Chemical potential

In DFT variational minimization of the energy functional, the associated Lagrange multiplier is identified with the chemical potential $\mu = (\partial E/\partial N)_{V(r)}$ and this is first order response of the energy changes with respect to the number of particles [36]. Though we are not dealing with open systems, the measurement of the escaping tendency of the whole electronic cloud is of great value for understanding the electron transfer processes during a chemical reaction. Numerical values of chemical potential are obtained using Eq. (3). The chemical potential obtained at different level of theory is given in Table 2. From the Fig. 3, it is found that chemical potential decreases gradually with increase in N—H distances and the TS has the intermediate value at both HF and DFT method. With increase in the level of theory, the chemical potential increases gradually up to TS and then it decreases. At both MP2 and QCISD method chemical potential increases with increase in N—H distances and reaches a maximum at the TS and then it gradually decreases.

The change in chemical potentials ($d\mu$) in double proton transfer of AAD at both HF and DFT method are calculated and found to be negative but that in both MP2 & QCISD method are found to be positive. From the concepts of thermodynamics it is known that the decrease in chemical potential in a chemical process make the reaction spontaneous. Higher level MP2 & QCISD calculations do not support the dimerization reaction in AAD. The results obtained at HF & well accepted DFT methods support the thermodynamic feasibility of the double proton transfer reaction in AAD (Scheme 1).This prompted us to use HF and DFT method to understand the mechanism of double proton transfer in AAD.

3.3. Ionization potential (IP), polarizability (α_{av}) and hardness (η)

The variations of polarizability, hardness, and ionization potential of acetamide dimerization reaction through double proton transfer are discussed in this section. The theoretical studies on the polarizability of double proton transfer reactions are not much in the literature. A recent study of Mandal et al. [37] on the polarizability for the dimers of formic acid ,acetic acid and trifluoro acetic acid along the proton transfer co-ordinate shows that the polarizability (at ω = 1064 nm) increases, reaches its maximum value at TS and then decreases. Our recent report [38] on formamide dimer, acetamide dimer and trifluoro acetamide dimer along the proton transfer co-ordinate suggests that the average polarizability is maximum and the chemical hardness is minimum at the transition state for all the three double proton transfer processes. Our present computation of polarizability (ω = 1064 nm) of AAD along its proton transfer co-ordinate using HF and DFT method reveals that the average polarizability values gradually increase from GS to TS and then decreases.

It is known that the static dipole polarizability is a measure of the distortion of the electronic density and the information about the response of the system under the influence of a static electric field. However, the ionization potential value predicts how tightly an electron is bound within the nuclear attractive field of the systems. A relationship between the polarizability and the ionization potential for atomic systems was first obtained by Dmitrieva and Plindov using a statistical model [39]. Fricke had shown that

Table 2
Chemical potential (a.u.) of AAD at various N—H distance using different level of theory.

r_{N-H} (Å)	HF/6-31G(d)	DFT-B3LYP/6-31G(d)	MP2/6-311G(d,p)	QCISD/6-31G(d)
1.00	−0.0975	−0.1065	−0.1225	−0.0990
1.05	−0.0975	−0.1065	−0.1225	−0.0985
1.10	−0.0975	−0.1070	−0.1225	−0.0978
1.15	−0.0975	−0.1075	−0.1210	−0.0976
1.20	−0.0980	−0.1095	−0.1195	−0.0976
1.25	−0.0985	−0.1110	−0.1190	−0.0973
1.30	−0.0990	−0.1120	−0.1185	−0.0970
1.35	−0.0995	−0.1130	−0.1190	−0.0990
1.40	−0.0995	−0.1135	−0.1190	−0.0995
1.45	−0.0995	−0.1140	−0.1190	−0.0997
1.50	−0.1000	−0.1140	−0.1195	−0.0995
1.55	−0.1000	−0.1145	−0.1200	−0.1003
1.60	−0.1005	−0.1150	−0.1210	−0.1003
1.65	−0.1005	−0.1150	−0.1215	−0.1005
1.70	−0.1005	−0.1155	−0.1220	−0.1008
1.75	−0.1005	−0.1155	−0.1220	−0.1008

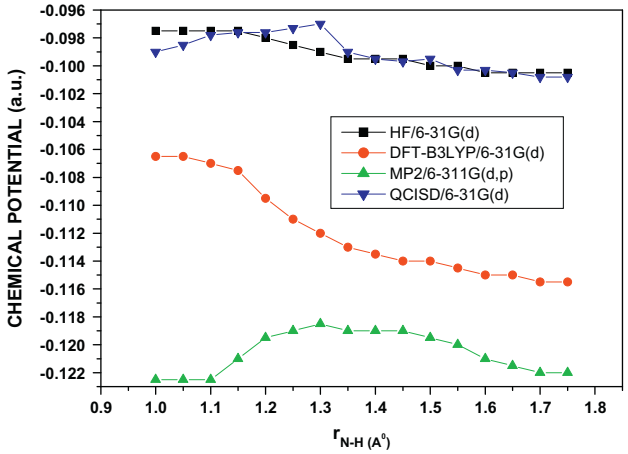

Fig. 3. Variation of chemical potential (a.u) with increasing N—H bond distances at different level of theory.

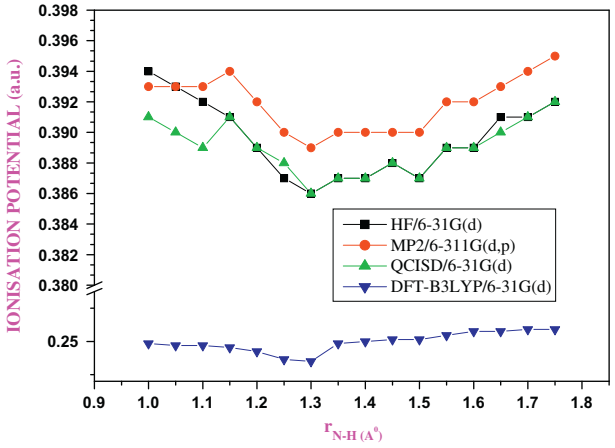

Fig. 4a. Variation of ionization potential (a.u) with increasing N—H bond distances at different level of theory.

polarizability of neutral atoms correlates very well with their first ionization potential (in a logarithmic scale) within the groups of elements with the same angular momentum of the outermost electrons [40]. In our present work, the variations of IP of the acetamide dimer along the reaction co-ordinate (r_{N-H}) calculated by HF, DFT, MP2 & QCISD methods are shown in Fig. 4a. The variation of average polarizability (α_{av}) at $\omega = 1064$ nm frequency with N—H distances in both HF & DFT methods are shown in Fig. 4b. The Fig. 4a reveals that in the course of acetamide dimerization reaction, the ionization potential decreases from GS to TS and reaches a minimum at TS and then increases. On the other hand average polarizability (Fig. 4b) increases from GS to TS and reaches a maximum value at TS and after TS it decreases with the further increase in N—H distance. One can indeed find that there is a good correlation between average polarizability and the inverse of ionization energy (IP^{-1}). From Figs. 4c and 4d it is found that IP decreases and average polarizability (α_{av}) increases along the proton transfer co-ordinate up to the transition state (TS). After the TS, IP increases and α_{av} decreases with increase in N—H distances. This is an important observation because the above results can provide a way to find out the polarizability of the dimeric

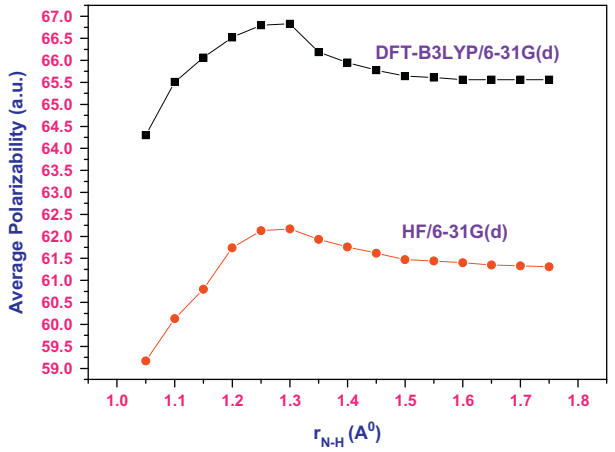

Fig. 4b. Variation of frequency dependent ($\omega = 1064$ nm) average polarizability (a.u) with increasing N—H bond distances at DFT and HF level of theory.

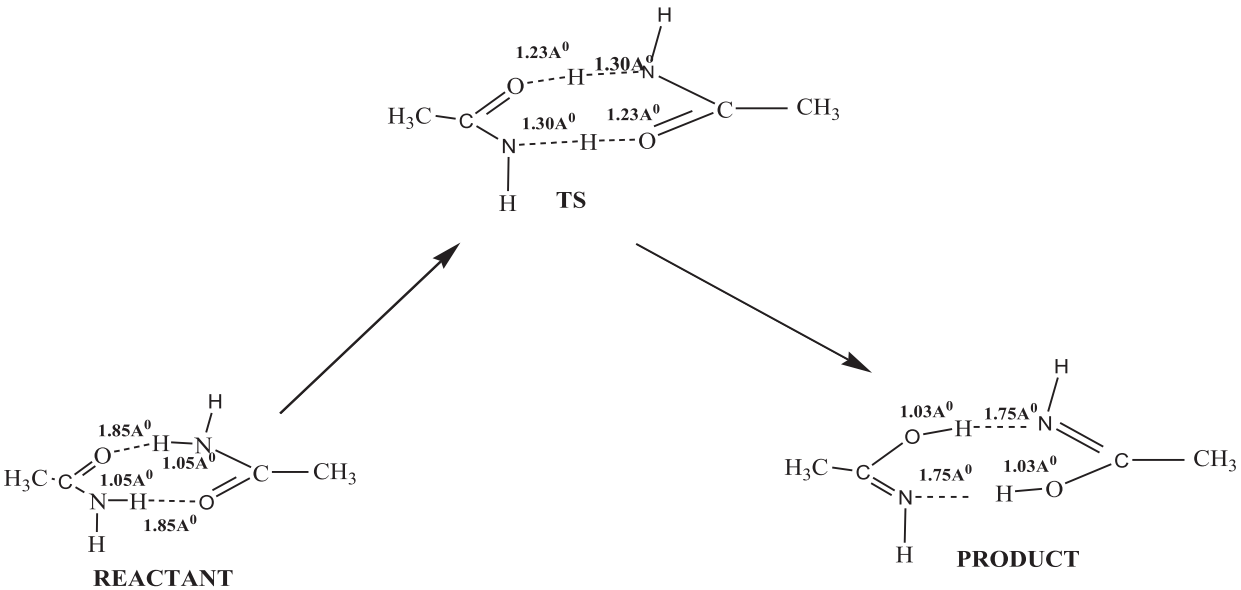

Scheme 1. Optimized structure of acetamide dimer (AAD) at GS, TS and Product using DFT-B3LYP/6-31G(d) level of theory.

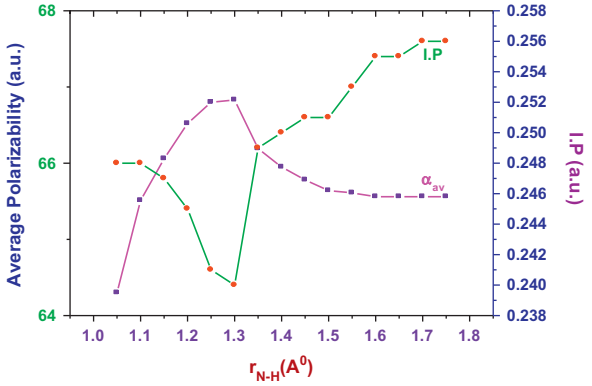

Fig. 4c. Variation of frequency dependent (ω = 1064 nm) average polarizability (a.u) and IP (a.u.) with increasing N—H bond distances at DFT-B3LYP/6-31G(d) level of theory.

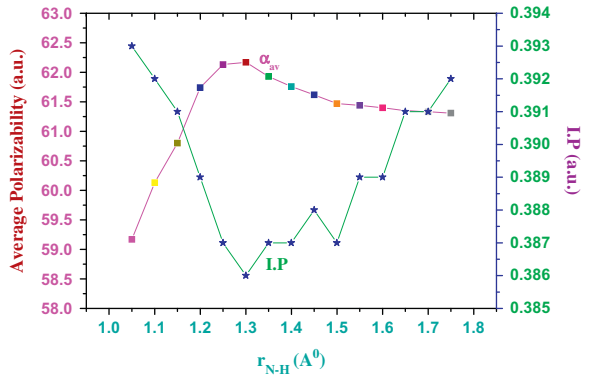

Fig. 4d. Variation of frequency dependent (ω = 1064 nm) average polarizability (a.u) and IP (a.u.) with increasing N—H bond distances at HF/6-31G(d) level of theory.

compounds from the values of their ionization potential along the double proton transfer reaction coordinate. This success in relating the polarizabilities to the ionization potential of the AAD would also be of interest in relating the ionization energies with average polarizability.

The global hardness parameter is inversely related to the polarizability of AAD system though this relation is mostly valid only for atomic systems. It is evident from Fig. 5a and Table 3 that the

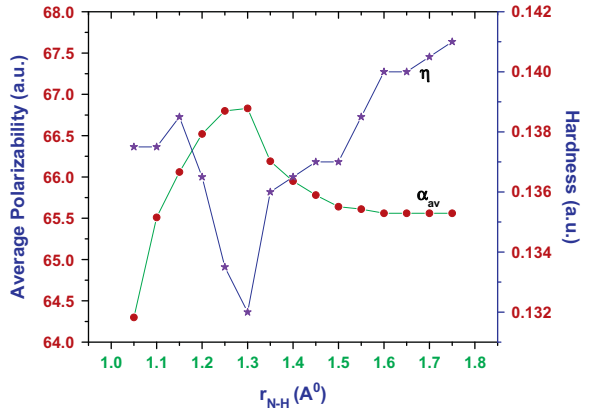

Fig. 5a. Variation of frequency dependent (ω = 1064 nm) average polarizability (a.u) and hardness (a.u.) with increasing N—H bond distances at DFT-B3LYP/6-31G(d) level of theory.

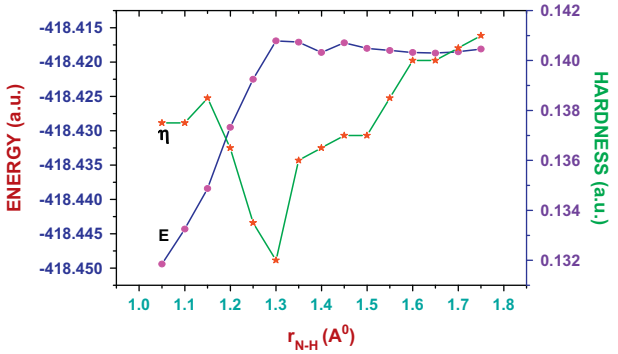

Fig. 5b. Variation of potential energy (E) (a.u) and hardness (a.u.) with increasing N—H bond distances at DFT-B3LYP/6-31G(d) level of theory.

Table 3
Variation of inter-action energy, average polarizability and chemical hardness with N—H distances (Å) using different level of theory.

	Interaction energy (kcal/mol)			Average polarizability (a.u.)		Chemical hardness (a.u.)	
r_{N-H} (Å)	HF/6-31G(d)	DFT/6-31G(d)	MP2/6-311G(d,p)	HF/6-31G(d)	DFT/6-31G(d)	HF/6-31G(d)	DFT/6-31G(d)
1.05	−13.07	−17.27	−15.2	59.17	64.3	0.2965	0.1375
1.1	−14.08	−19.6	−17.42	60.13	65.51	0.2945	0.1375
1.15	−15.73	−24.42	−22.78	60.8	66.06	0.2935	0.1385
1.2	−17.82	−29.4	−28.8	61.74	66.52	0.291	0.1365
1.25	−21.39	−36.94	−38.38	62.13	66.8	0.2885	0.1335
1.3	−28.79	−47.34	−50.84	62.17	66.83	0.287	0.132
1.35	−41.26	−59.69	−64.95	61.93	66.19	0.2875	0.136
1.4	−57	−73.04	−79.79	61.76	65.95	0.2875	0.1365
1.45	−74.23	−86.75	−94.81	61.62	65.78	0.288	0.137
1.5	−91.98	−100.56	−109.94	61.47	65.64	0.2875	0.137
1.55	−110.86	−113.79	−124.04	61.44	65.61	0.289	0.1385
1.6	−127.12	−126.55	−137.64	61.4	65.56	0.289	0.14
1.65	−160.32	−139.03	−151.08	61.35	65.56	0.2905	0.14
1.7	−175.93	−150.79	−163.2	61.33	65.56	0.291	0.1405
1.75	−190.88	−161.92	−175.44	61.31	65.56	0.2915	0.141

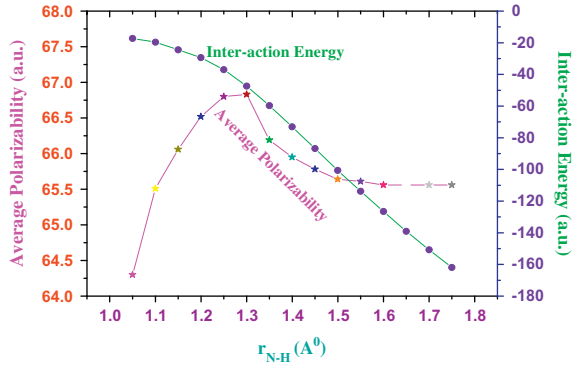

Fig. 6a. Variation of frequency dependent (ω = 1064 nm) average polarizability (a.u) and interaction energy (a.u.) with increasing N—H bond distances at DFT-B3LYP/6-31G(d) level of theory.

chemical hardness (η) and average polarizability (α_{av}) of the AAD are inversely related to each other. Hence one can approximate the global hardness parameter in terms of ionization potential alone. It further explain that the polarizability correlates nicely with the softness ($1/\eta$) parameter as well as ionization potential.

From Fig. 5b, it is found that the chemical hardness (η) is also inversely related with energy (E) of the AAD. At TS energy is

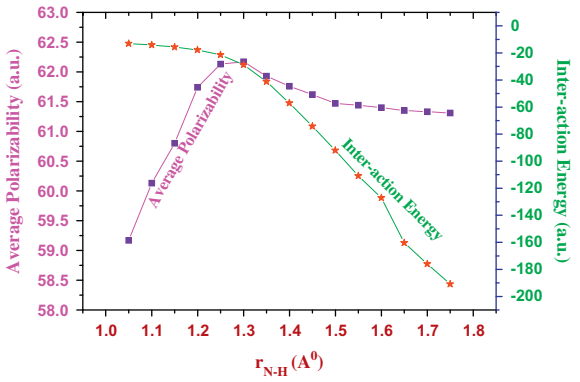

Fig. 6b. Variation of frequency dependent ($\omega = 1064$ nm) average polarizability (a.u) and interaction energy (a.u.) with increasing N—H bond distances at HF/6-31G(d) level of theory.

maximum and hardness is minimum. This implies that the most unstable structure is associated with TS structure along the reaction co-ordinate. Thus TS may be defined as a molecular structure which has maximum energy, maximum polarizability, minimum hardness and minimum ionization energy.

From the above arguments, the physical basis for the relationship among the energy, average polarizability and the softness as well as the inverse of ionization potential can be rationalized. Herein, we have, however, shown that this relationship can be validated for the other dimeric system as well. The analytical proof of the above relation is, however, yet to be studied for several molecular systems.

3.4. Interaction energy

The interaction energy (IE in kcal mol^{-1}) for AAD is calculated as shown below.

$$\mathrm{IE} = E_{\mathrm{total}} - n \cdot E_{\mathrm{monomer}} \quad (9)$$

E_{total} is the energy of the dimmer; E_{monomer} the energy of acetamide monomer; and n is the number of acetamide unit.

We have calculated the IE using different methods along the proton transfer coordinate and it has been listed in Table 3. Our calculation shows that the value of IE ranges from −13.0712 to −190.8897 kcal mol^{-1} for reactant and product respectively.

Recent studies investigating the physical properties of the van der Waals coefficients (a and b) and their correlation with the polarizability volume (α) show how the intermolecular interaction energy correlates with the polarizability volume of molecules [41]. In the present context we have plotted the polarizability (α_{av}) and interaction energy (IE) of the acetamide dimer along the proton transfer co-ordinate using DFT and HF methods as shown in Figs. 6a and 6b. The list of α_{av} and IE values at different N—H distances are given in Table 3. These plots reveal that there is a clear increase in the polarizability of AAD with decrease in interaction energy up to TS and after the TS polarizability decreases with decreased in interaction energy. During the course of double proton transfer reaction in AAD the distance between donor, nitrogen and acceptor, oxygen and all other bond parameters remain almost same, but the N—H distance changes. When H comes from N-end to TS, α_{av} sharply increases with dercrease in IE. This approach maintains the inverse relationship between α_{av} and IE. But after TS when H comes to more electronegative O-end, the departure from inverse relationship between α_{av} and IE occurs. It may be assumed that the departure from inverse relationship occur due to formation of H-bond. After the TS the formation of H-bond takes place. Due to stronger inter-molecular H-bonding tendency between two acetamide molecules the interaction energy decreases. Thus, for the presence of stronger inter-molecular H-bonding capacity, polarizability decreases by keeping the inter-molecular distances (Donor–Acceptor) same in the course of dimerization reaction.

4. Conclusion

The study of energy force profile and other reactivity parameters of the titled dimeric molecule as a function of inter-molecular rearrangement of two hydrogen atoms provide an insight into the ground state proton-transfer processes in acetamide dimer. It is shown that the degree of cationization of the ground state acetamide dimer is low compare to the transition state structure along the proton transfer path. It has also been concluded that the energetically stable structure is associated with higher ionization potential and lower polarizability. It has been shown that the energetically most stable proton-transferred structure is associated with maximum hardness. In order to get further insight in the mechanism of double proton transfer processes, the parameters like energy, hardness, polarizability, ionization potential, chemical potential and interaction energy along the reaction co-ordinates have been computer along the proton transfer path. The activation energy for the double proton transfer process is shown to have direct correlation with the parameter like polarizability, hardness and ionization potential. Also, the study of these parameters further strengthens the principles of maximum hardness and minimum polarizability to substantiate the double proton transfer path in acetamide dimer.

Acknowledgements

We gratefully acknowledge the financial support received from CSIR, New Delhi (Ref. No. 01(2443)/10/EMR-II) and University Grant Commission (UGC), New Delhi for carrying out this research work. We are thankful to USIC, Vidyasagar University for providing Gaussian-09 software. We are also thankful to Prof. Swapan Kr. Pati, JNCASR Bangalore for helpful discussions.

References

[1] L. Melander, W.H. Saunders, Reaction Rates of Isotopic Molecules, John Wiley & Sons, New York, 1980.
[2] G.A. Jeffrey, W. Saenger, Hydrogen-Bonding in Biological Structures, Springer-Verlag, Berlin, 1991.
[3] (a) Ke-Li Han, Guang-Jiu Zhao, Hydrogen Bonding and Transfer in the Excited State, vol. 2, John Wiley & Sons, UK, 2011;
(b) S. Scheiner, Hydrogen Bonding: A Theoretical Perspective, Oxford University Press, New York, 1997.
[4] (a) S.P. De, S. Ash, S. Dalai, A. Misra, A DFT-based comparative study on the excited states intramolecular proton transfer in 1-hydroxy-2-naphthaldehyde and 2-hydroxy-3-naphthaldehyde, J. Mol. Struct. (THEOCHEM) 807 (2007) 33–41;
(b) B. Herrera, A. Toro-Labbe, Theoretical study of the HXNY → XNYH (X, Y = O, S) intramolecular proton transfer reactions, J. Phys. Chem. A. 108 (2004) 1830–1836.
[5] P. Jaque, A. Toro-Labbe, Theoretical study of the double proton transfer in the CHX-XH---CHX-XH (X = O, S) complexes, J. Phys. Chem. A 104 (2000) 995–1003.
[6] (a) S.P. De, S. Ash, H.K. Bar, D.K. Bhui, P. Sarkar, G.P. Sahoo, A. Misra, DFT based computational study on the excited state intramolecular proton transfer processes in o-hydroxybenzaldehyde, Spectrochim. Acta Part A. 71 (2009) 1728–1735;
(b) P. Brzezinski, Proton transfer reactions in bioenergetics, Biochim. Biophys. Acta 1458 (2000) 1–219.
[7] (a) S. Ash, S.P. De, H. Beg, A. Misra, Excited state intramolecular proton transfer in 3-hydroxychromone: a DFT-based computational study, Mol. Simul. 37 (2011) 914–922;
(b) L.I. Krishtalik, The mechanism of the proton transfer: an outline, Biochim. Biophys. Acta 1458 (2000) 6–27.
[8] (a) J.C. Kendrew, R.E. Dickerson, B.E. Strandberg, R.G. Hart, D.R. Davis, D.C. Philips, V.G. Shore, Structure of myoglob: a three-dimensional Fourier synthesis at 2 Å resolution, Nature 185 (1960) 422–427;

(b) G.E. Schultz, R.H. Schrimer, Principles of Protein Structure, Springer-Verlag, New York, 1979.

[9] (a) I.M. Klotz, J.S. Franzen, Hydrogen bonds between model peptide groups in solution, J. Am. Chem. Soc. 84 (1962) 3461–3466;
(b) H. Susi, S.N. Timasheff, J.S. Ard, Near infrared investigation of interamidehydrogen bonding in aqueous solution, J. Biol. Chem. 239 (1964) 3051–3054;
(c) H.E. Affsprung, S.D. Christian, J.D. Worley, Self association of c-butyrolactam in CCl4, Spectrochim. Acta 20 (1964) 1415–1429;
(d) H. Susi, Hydrogen bonding of amide groups in dioxane solution, J. Phys. Chem. 69 (1965) 2799–2801;
R.F.W. Hopmann, Chemical relaxation as a mechanistic probe of hydrogen bonding. thermodynamics and kinetics of lactam isoassociation in nonpolar solvents, J. Phys. Chem. 78 (1974) 2341–2348;
J.A. Walmsley, Self-association of 2-pyrrolidinone. 2. Spectral and dielectric polarization studies of benzene solutions, J. Phys. Chem. 82 (1978) 2031–2035;
C. Josefiak, G.M. Schneider, Determination of reaction volumes of hydrogen-bonding equilibriums by high pressure near-infrared spectroscopy. 1. Self-association of epsilon-caprolactam in tetrachloromethane up to 2 kbar, J. Phys. Chem. 83 (1979) 2126–2128;
(h) S.E. Krikorian, Determination of dimerization constants of cis- and transconfigured secondary amides using near-infrared spectrometry, J. Phys. Chem. 86 (1982) 1875–1881;
(i) M.S. Searle, D.H. Williams, U. Gerhard, Partitioning of free energy contributions in the estimation of binding constants: residual motions and consequences for amide–amide hydrogen bond strengths, J. Am. Chem. Soc. 114 (1992) 10697–10704.

[10] P. Hobza, F. Mulder, C. Sandorfy, Quantum chemical and statistical thermodynamic investigations of anesthetic activity. 2. The interaction between chloroform, fluoroform, and an N—H---O—C hydrogen bond, J. Am. Chem. Soc. 104 (1982) 925–928;
(b) W.L. Jorgensen, Interactions between amides in solution and the thermodynamics of weak binding, J. Am. Chem. Soc. 111 (1989) 3770–3771.

[11] S.C. Moldoveanu, Analytical Pyrolysis of Natural Organic Polymers, in: Techniques and Instrumentation in Analytical Chemistry, Elsevier, Amsterdam, 1998.

[12] E. T Mirkova, Activities of the rodent carcinogens thioacetamide and acetamide in the mouse bone marrow micronucleus assay, Mutat. Res. 352 (1996) 23–30.

[13] X. Song, S.J. Farwell, Pyrolysis gas chromatography atomic emission detection method for determination of N-containing components of humic and fulvic acids, Anal. Appl. Pyrolysis 71 (2004) 901–915.

[14] G.S. Lal, E.R. Hayes, Determination of the amine content of chitosan by pyrolysisgas chromatography, J. Anal. Appl. Pyrolysis 6 (1984) 183–193.

[15] H.R. Buser, M. Muller, Environmental behavior of acetamide pesticide sterioisomers. 2. Stereo- and enantioselective degradation in sewage sludge and-soil, Environ. Sci. Technol. 29 (1995) 2031–2037.

[16] J. Yinon, R. Yost, S. Bulusub, Thermal decomposition characterization of explosives by pyrolysis-gas chromatography–mass spectrometry, J. Chromatogr. A. 688 (1994) 231–242.

[17] L. Berwick, P. Greenwood, R. Kagi, Croue, Thermal release of nitrogen organics from natural organic matter using micro scale sealed vessel pyrolysis, J.P. Org. Geochem. 38 (2007) 1073–1090.

[18] R.K. Sharma, W.G. Chan, On the role of peptides in the pyrolysis of amino acids, J. Anal. Appl. Pyrolysis 72 (2004) 153–163.

[19] H. Schmidt, F.K. Tadjimukhamedov, K.M. Douglas, S. Prasad, G.B. Smith, G.A. Eiceman, Quantitative assessment and optimization of parameters for pyrolysis of bacteria with gas chromatographic analysis, J. Anal. Appl. Pyrolysis 76 (2006) 161–168.

[20] T.P. Das, E.L. Han, Nuclear Quadrupole Resonance Spectroscopy, Academic Press, New York, 1958.

[21] F.A. Bovey, Nuclear Magnetic Resonance Spectroscopy, Academic Press, San Diego, 1988.

[22] (a) Z. Samadi, M. Mirzaei, N.L. Hadipour, S. Abedini Khorami, Density functional calculations of oxygen, nitrogen and hydrogen electric field gradient and chemical shielding tensors to study hydrogen bonding properties of peptide group (O═C—NH) in crystalline acetamide, J. Mol. Graph. Model. 26 (2008) 977;
(b) M. Albrecht, C.A. Rice, M.A. Suhm, Elementary peptide motifs in the gas phase: FTIR aggregation study of formamide, acetamide, N-methylformamide, and N-methylacetamide, J. Phys. Chem. A 112 (2008) 7530–7542;
(c) L.C. Maynet, B. Hudson, Resonance Raman spectroscopy of IV-methyiacetamide: overtones and combinations of the C—N stretch (Amide 11') and effect of solvation on the C═O stretch (Amide I) intensity, J. Phys. Chem. 95 (1991) 2961–2962;
(d) T.M. Watson, J.D. Hirst, Density functional theory vibrational frequencies of amides and amide dimers, J. Phys. Chem. A 106 (2002) 7858–7867;
(e) W.L. Jorgensen, J. Gao, Cis–trans energy difference for the peptide bond in the gas phase and in aqueous solution, J. Am. Chem. Soc. 110 (1988) 4212–4216;
(f) M.D. Esrafili, H. Behzadi, N.L. Hadipour, Theoretical study of N—H• • •O hydrogen bonding properties and cooperativity effects in linear acetamide clusters, Theor. Chem. Acc. 121 (2008) 135–146;
(g) J.C. Hargis, E.V. Martinez, H.L. Woodcock, A. Toro-Labb, H.F. Schaefer, Characterizing the mechanism of the double proton transfer in the formamide dimer, J. Phys. Chem. A 115 (2011) 2650–2657.

[23] (a) P.K. Chattaraj, P. Fuentealba, P. Jaque, A. Toro-Labbe, Validity of the minimum polarizability principle in molecular vibrations and internal rotations: an ab initio SCF study, J. Phys. Chem. A. 103 (1999) 9307–9312;
(b) G.I. Cfirdenas-Jiront, A. Toro-Labbe, Hardness profile and activation hardness for rotational isomerization processes. 2. The maximum hardness principle, J. Phys. Chem. 99 (1995) 12730–12738.

[24] (a) S. Sengupta, A. Toro-Labbe, Estimating molecular electronic chemical potential and hardness from fragments addition schemes, J. Phys. Chem. A 106 (2002) 4443–4446;
(b) R.G. Pearson, Chemical Hardness: Applications from Molecules and Solids, Wiley-VCH Verlag GMBH, Weinheim, Germany, 1997;
(c) R.G. Parr, R.G. Pearson, Absolute hardness: companion parameter to absolute electronegativity, J. Am. Chem. Soc. 105 (1983) 7512–7516;
(d) R.G. Parr, W. Yang, Density Functional Theory of Atoms and Molecules, Oxford University Press, New York, 1989;
(e) K.D. Sen (Ed.), Structure and Bonding, Chemical Hardness, vol. 80, Springer-Verlag, Berlin, Germany, 1993.

[25] T.K. Ghanty, S.K. Ghosh, A density functional approach to hardness, polarizability, and valency of molecules in chemical reactions, J. Phys. Chem. 100 (1996) 12295–12298.

[26] T. Mineva, E. Sicilia, N. Russo, Density-functional approach to hardness evaluation and its use in the study of the maximum hardness principle, J. Am. Chem. Soc. 120 (1998) 9053–9058.

[27] T. Mineva, V. Parvanov, I. Petrov, N. Neshev, N. Russo, Fukui indices from perturbed Kohn–Sham orbitals and regional softness from Mayer atomic valences, J. Phys. Chem. A. 105 (2001) 1959–1967.

[28] G. De Luca, E. Sicilia, N. Russo, T. Mineva, On the hardness evaluation in solvent for neutral and charged systems, J. Am. Chem. Soc. 124 (2002) 1494–1499.

[29] N. Russo, M. Toscano, A. Grand, T. Mineva, Proton affinity and protonation sites of aniline. Energetic behavior and density functional reactivity indices, J. Phys. Chem. A 104 (2000) 4017–4021;
(b) T. Mineva, N. Russo, Atomic Fukui indices and orbital hardnesses of adenine, thymine, uracil, guanine and cytosine from density functional computations, J. Mol. Struct. (THEOCHEM) 943 (2010) 71–76.

[30] A. Toro-Labbe, S. Gutierrez-Oliva, M.C. Concha, J.S. Murray, P. Politzer, Analysis of two intramolecular proton transfer processes in terms of the reaction force, J. Chem. Phys. 121 (2004) 4570–4576.

[31] A.D. Becke, Density-functional thermochemistry. III. The role of exact exchange, J. Chem. Phys. 98 (1993) 5648–5652;
(b) C. Lee, W. Yang, R.G. Parr, Development of the Colle–Salvetti conelation energy formula into a functional of the electron density, Phys. Rev. B 37 (1988) 785–789.

[32] P.C. Hariharan, J.A. Pople, The influence of polarization functions on molecular orbital hydrogenation energies, Theor. Chem. Acta 28 (1973) 213–222.

[33] M.J. Frisch et al., Gaussian 09, Gaussian, Inc., Wallingford, CT, 2009.

[34] (a) S.J.A. van Gisbergen, J.G. Snijders, E. Baerends, Time-dependent density functional results for the dynamic hyperpolarizability of C60, J. Phys. Rev. Lett. 78 (1997) 3097–3100;
(b) S.J.A. van Gisbergen, J.G. Snijders, E.J. Baerends, Calculating frequency dependent hyperpolarizabilities using time-dependent density functional theory, J. Chem. Phys. 109 (1998) 10644–10656.

[35] (a) G. Maroulis, P. Karamanis, C. Pouchan, Hyperpolarizability of GaAs dimer is not negative, J. Chem. Phys. 126 (2007) 154316–1543165;
(b) G. Maroulis, How large is the static electric (hyper) polarizability anisotropy in HXeI?, J Chem Phys. 129 (2008) 44314–44317;
(c) P. Karamanis, C. Pouchan, G. Maroulis, Structure, stability, dipole polarizability and differential polarizability in small gallium arsenide clusters from all-electron ab initio and density–functional–theory calculations, Phys. Rev. A 77 (2008) 13201–13207.

[36] K.D. Sen, C. Joegensen (Eds.), Structure and Bonding: Electronegativity, vol. 66, Springer-Verlag, Berlin, 1987.

[37] T.K. Mandal, S.K. Pati, Ayan Dutta, Degenerate intermolecular and intramolecular proton-transfer reactions: electronic structure of the transition states, J. Phys. Chem. A 113 (2009) 8147–8151.

[38] H. Beg, S.P. De, S. Ash, A. Misra, Use of polarizability and chemical hardness to locate the transition state and the potential energy curve for double proton transfer reaction: a DFT based study, Comput. Theor. Chem. 984 (2012) 13–18.

[39] I.K. Dmitrieva, G. Plindov, Dipole polarizability, radius and ionization potential for atomic systems, I. Phys. Scr. 27 (1983) 402–406.

[40] B. Fricke, On the correlation between electric polarizabilities and the ionization potential of atoms, J. Chem. Phys. 84 (1986) 862–866.

[41] (a) S.P. de Visser, Van der Waals equation of state revisited: importance of the dispersion correction, J. Phys. Chem. B 115 (2011) 4709–4717;
(b) S.P. de Visser, On the relationship between internal energy and both the polarizability volume and the diamagnetic susceptibility, Phys. Chem. Chem. Phys. 1 (1999) 749–753.